J. Cent. South Univ. (2015) 22: 2348−2358
DOI: 10.1007/s11771-015-2760-y

Springer

An improved multidirectional velocity model for micro-seismic monitoring in rock engineering

LI Jian(李健)[1, 2], WU Shun-chuan(吴顺川)[1], GAO Yong-tao(高永涛)[1], LI Li-jie(李莉洁)[3], ZHOU Yu(周喻)[1]

1. Key Laboratory of Efficient Mining and Safety of Metal Mine of Ministry of Education (University of Science and Technology Beijing), Beijing 100083, China;
2. School of Civil and Resource Engineering, University of Western Australia, 35 Stirling Highway, Crawley, WA 6009, Australia;
3. State Key Laboratory of Rail Traffic Control and Safety (Beijing Jiaotong University), Beijing 100044, China

Abstract: An improved multidirectional velocity model was proposed for more accurately locating micro-seismic events in rock engineering. It was assumed that the stress wave propagation velocities from a micro-seismic source to three nearest monitoring sensors in a sensor's array arrangement were the same. Since the defined objective function does not require pre-measurement of the stress wave propagation velocity in the field, errors from the velocity measurement can be avoided in comparison to three traditional velocity models. By analyzing 24 different cases, the proposed multidirectional velocity model iterated by the Simplex method is found to be the best option no matter the source is within the region of the sensor's array or not. The proposed model and the adopted iterative algorithm are verified by field data and it is concluded that it can significantly reduce the error of the estimated source location.

Key words: multidirectional velocity model; micro-seismic event; Simplex method; rock engineering; field measurement; error estimation

1 Introduction

Most solids emit low-level seismic signals when they are stressed or deformed. A variety of terms, including acoustic emission, micro-seismic activity, seism-acoustic activity and micro-earthquake activity have been utilized by different disciplines to describe this phenomenon. In the fields of engineering geology and rock engineering, it is termed to be a micro-seismic/acoustic emission (MS/AE) event [1]. Related technologies in monitoring the MS/AE events have become more and more important in assessing the stability of a rock mass, and they have been increasingly applied in the engineering fields including mining [2], hydropower dam [3], tunnel excavation [4] and other industries after years of development. In practical rock engineering, a micro-seismic event refers to the majority frequencies of the induced seismic waves within the range from 10 Hz to 10^3 Hz.

The effectiveness of the micro-seismic monitoring technology greatly depends on the accuracy level that can be achieved in estimating the event location. Due to the existence of joints and fissures in a rock mass, attenuation of energy and velocity of a seismic wave inevitably occurs in the process of stress wave propagation. With the combined influence of all the reflections and refractions at the inherent discontinuities, a considerable positioning error in estimating the micro-seismic source location is often produced. To achieve higher precision positioning, a reasonable sensors' array configuration and associated filtering and waveform identification technique have been suggested [5]. In the process, adoption of a suitable micro-seismic source locating method is critical. Over the years, lots of fruitful research has been carried out on this topic by scholars around the world. The existing source locating algorithms can be divided into two categories, i.e., the non-iterative algorithm and the iterative algorithm, as shown in Fig. 1. Among different non-iterative algorithms, the triaxial approach [6] and the zonal location method [7] are highly influenced by the geologic structure and characteristic of the rock material. Other early and widely used non-iterative algorithms include the INGLADA [8], the USBM algorithm [9] and so on. When the number of sensors is more than five, the

Foundation item: Project(IRT0950) supported by the Cheung Kong Scholars and the Development Plan of Innovative Team, China; Project supported by China Scholarship Council
Received date: 2014−05−17; **Accepted date:** 2014−10−11
Corresponding author: WU Shun-chuan, Professor, PhD; Tel: +86−10−62333623; E-mail: wushunchuan@ustb.edu.cn

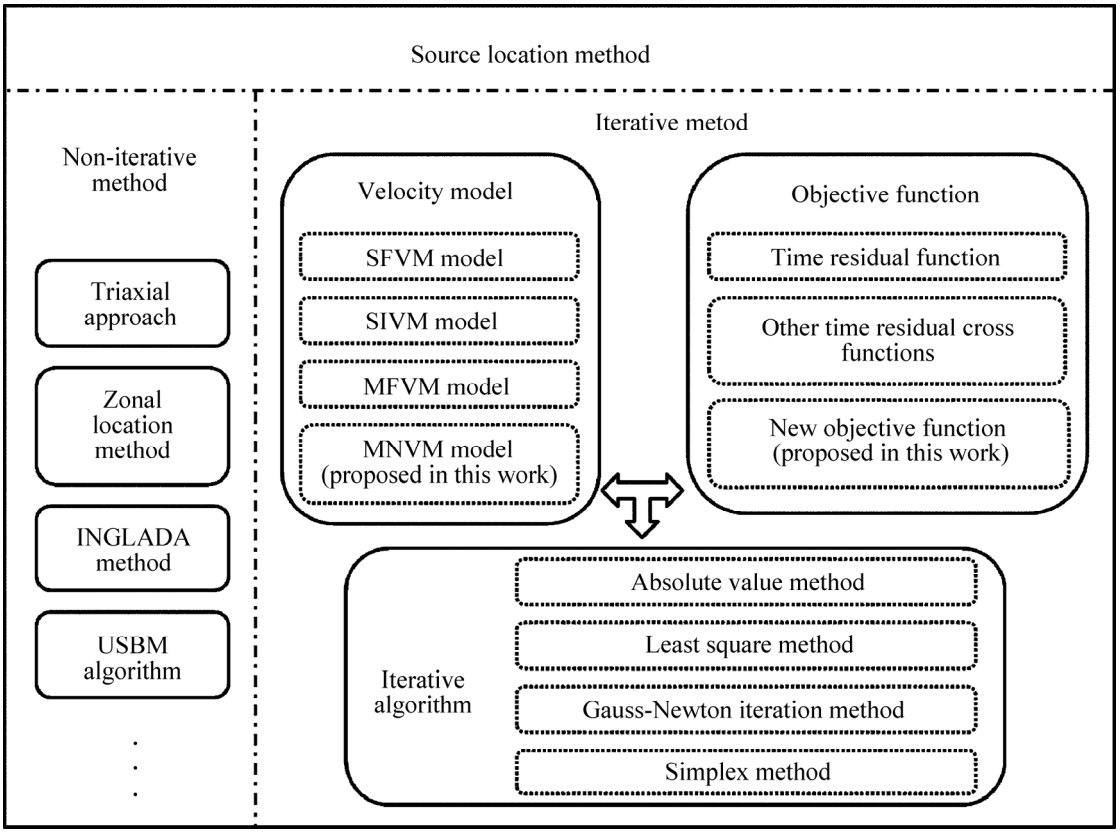

Fig. 1 Location principles based on different velocity model

stress wave propagation velocity can be treated as an additional unknown. The non-iterative algorithm has advantage when the field measured data are reliable. However, the inevitable error of the data collected by sensors in practical engineering often leads to an unacceptable positioning accuracy. Besides, the number of nonlinear equations will increase drastically when the quantity of waves picked by the sensors is large. In this case, it will be difficult to accurately determine the location of micro-seismic event.

On the other hand, an iterative algorithm is more suitable in finding the best approximation of the event location when the measured data have a certain degree of uncertainties. The implementation of an iterative algorithm requires selecting a proper velocity model and its associated objective function in minimizing errors. The commonly used velocity models include the field measurement based single velocity model, the inversion based single velocity model, and the field measurement based multidirectional velocity model. The difference of the field measurement and inversion based models is that the former uses pre-measured wave propagation velocity or velocities while the later considers the wave velocity as unknown in the analysis. A single velocity model assumes that the wave propagation velocities to different sensors are the same, while they can be different based on the multidirectional velocity model. Corresponding objective functions include the time residual function and the time residual cross functions, etc. The iterative algorithms can also be classified into the minimum absolute value method [10], the least square method [11], the Gauss-Newton iterative method [12] or the Geiger method [13], the Simplex method, and so on. Specifically, CHRISTY [14] and STRANG [15] respectively combined the INGLADA method and the USBM method with the least square method based on the single velocity model, which achieved better results than the non-iterative method. VANDECAR and CROSSON [16], MENKE [17], LI and DONG [18] introduced time residual cross functions as new objective functions in the iterative algorithm based on the single velocity model. AKI and LEE [19] put forward the theory of 3D inversion combining velocity and source. PAVLIS and BOOKER [20] made an improvement by separating the unknown velocities from the coordinates of source in the objective function. BULAND [12] used a Gauss-Newton iterative method to search the source with the multidirectional velocity model based on field velocity measurement. THURBER [21] proposed a residual to the second order for the objective function and solved the solution by iterations. PRUGGER and GENDZWILL [22] used Simplex method [23] to obtain the solution with the multidirectional velocity model. WALDHAUSER and ELLSWORTH [24] proposed a double difference

location method with the objective function of the same sensor's residual function of different events.

Since the stress wave propagation velocity from a micro-seismic source to different sensors may be different and the velocity models highly rely on the accuracy of the pre-measured stress wave propagation velocity at field or the applied inversion velocity, errors are always inevitable in practical micro-seismic monitoring. In order to reduce such error and more accurately locate the micro-seismic events in a rock mass, a new multidirectional velocity model without velocity inversion or pre-measurement of field velocity is proposed in this work. 24 different cases are analyzed with the proposed multidirectional velocity model iterated by the Simplex method. The proposed model and the adopted iterative algorithm are verified by field data.

2 Traditional velocity models in micro-seismic monitoring

Micro-seismic sensors to pick up stress waves induced by rock fracturing are set up with a certain array arrangement in the three-dimensional space. They are normally embedded in boreholes in rock. For each sensor i (i=1, 2, 3, ⋯, n), assuming that the stress wave propagation velocity from a MS source is v_i (i=1, 2, 3, ⋯, n), the three-dimensional coordinates of the sensor i and the MS source are (x_i, y_i, z_i) and (x_0, y_0, z_0), respectively, t_i is the arrival time of stress waves from the MS source to the sensor i, and t_0 is the origin time, it has the relation:

$$\sqrt{(x_i-x_0)^2+(y_i-y_0)^2+(z_i-z_0)^2}=v_i(t_i-t_0) \tag{1}$$

Assuming that the calculated coordinates of the source is (x_0', y_0', z_0') during the iteration process, where the origin time is t_0', the velocity from the estimated source to the sensor i is v_t', the arrival time t_{ci} from the estimated source to the sensor i can be calculated by

$$t_{ci}=\frac{\sqrt{(x_i-x_0')^2+(y_i-y_0')^2+(z_i-z_0')^2}}{v_i'} \tag{2}$$

The residual time γ_i for each sensor i is then given by

$$\gamma_i=t_i-t_{ci}-t_0' \tag{3}$$

And the objective function for each coordinate of source (x_0', y_0', z_0') is

$$\sum_{i=1}^{n}\gamma_i^2=\sum_{i=1}^{n}(t_i-t_{ci}-t_0')^2=\sum_{i=1}^{n}[t_i-((x_i-x_0')^2+(y_i-y_0')^2+(z_i-z_0')^2)^{1/2}/v_i'-t_0']^2 \tag{4}$$

The traditional iterative algorithms aimed to minimize the objective function in Eq. (4) based on different velocity models. As the velocity v_t' from each source to different sensors can be different, three velocity models and corresponding objective functions have been suggested.

1) Field measurement based single velocity model

Assuming that the velocities from a MS source to different sensors have the same value of v_{K1}, which is determined by field measurement near the area of the MS source, the objective function in Eq. (4) can be rewritten as

$$\sum_{i=1}^{n}\gamma_i^2=\sum_{i=1}^{n}[t_i-((x_i-x_0')^2+(y_i-y_0')^2+(z_i-z_0')^2)^{1/2}/v_{K1}-t_0']^2 \tag{5}$$

Since there are three unknowns only in Eq. (5), at least three sensors are required to locate the MS source based on this model. The effectiveness of this model depends on the accuracy of the pre-measured velocity v_{K1} and the homogeneity of the rock mass.

2) Inversion based single velocity model

Assuming that the velocities from a MS source to different sensors have the same value v_{K1}', which is assumed to be an additional unknown just like the coordinates of an MS source, the objective function is changed to be

$$\sum_{i=1}^{n}\gamma_i^2=\sum_{i=1}^{n}[t_i-((x_i-x_0')^2+(y_i-y_0')^2+(z_i-z_0')^2)^{1/2}/v_{K1}'-t_0']^2 \tag{6}$$

Due to the fact that the additional known, i.e. v_{K1}', is introduced, at least four sensors are required based on this model. The disadvantage of this model is that the rock mass is also assumed to be homogenous.

3) Field measurement based multidirectional velocity model

Assuming that the velocities from different sources to sensor i have the same value v_{Ki}, which is determined by field measurements near the area of potential MS sources, the objective function then becomes

$$\sum_{i=1}^{n}\gamma_i^2=\sum_{i=1}^{n}[t_i-((x_i-x_0')^2+(y_i-y_0')^2+(z_i-z_0')^2)^{1/2}/v_{Ki}-t_0']^2 \tag{7}$$

Obviously, the accuracy of this model highly relies on the field measurement of velocities v_{Ki}, which is dependent on the accuracy of the estimations of the MS sources.

Besides the objective functions given in Eq. (4) to Eq. (7), other kinds of objective functions have also been proposed [16−18, 24]. Due to space limit, details of the coupled velocity models and their corresponding objective functions are not introduced here.

3 A new multidirectional velocity model

Assuming that the wave velocities from a MS source to sensor j and two sensors k and u, which are the nearest sensors to sensor j, have the same value v_j, the arrival times to sensors j, k and u are

$$t_j = \frac{\sqrt{(x_j - x_0')^2 + (y_j - y_0')^2 + (z_j - z_0')^2}}{v_j} + t_0' \tag{8}$$

$$t_k = \frac{\sqrt{(x_k - x_0')^2 + (y_k - y_0')^2 + (z_k - z_0')^2}}{v_j} + t_0' \tag{9}$$

$$t_u = \frac{\sqrt{(x_u - x_0')^2 + (y_u - y_0')^2 + (z_u - z_0')^2}}{v_j} + t_0' \tag{10}$$

Let

$$D_j = \sqrt{(x_j - x_0')^2 + (y_j - y_0')^2 + (z_j - z_0')^2} \tag{11}$$

$$D_k = \sqrt{(x_k - x_0')^2 + (y_k - y_0')^2 + (z_k - z_0')^2} \tag{12}$$

$$D_u = \sqrt{(x_u - x_0')^2 + (y_u - y_0')^2 + (z_u - z_0')^2} \tag{13}$$

When Eq. (8) is respectively subtracted by Eq. (9) and Eq. (10), it has

$$t_j - t_k = (D_j - D_k)/v_j \tag{14}$$

$$t_j - t_u = (D_j - D_u)/v_j \tag{15}$$

1) If $t_j \neq t_k \neq t_u$, then

$$v_j = (D_j - D_k)/(t_j - t_k) = (D_j - D_u)/(t_j - t_u) \tag{16}$$

Taking the right side of the equation to the left, then

$$(D_j - D_k)/(t_j - t_k) - (D_j - D_u)/(t_j - t_u) = 0 \tag{17}$$

For sensor j,

$$\begin{aligned} R_j = {} & [(D_j - D_k)/(t_j - t_k) - (D_j - D_u)/(t_j - t_u)]^2 + \\ & [(D_k - D_j)/(t_k - t_j) - (D_k - D_u)/(t_k - t_u)]^2 + \\ & [(D_u - D_j)/(t_u - t_j) - (D_u - D_k)/(t_u - t_k)]^2\} \end{aligned} \tag{18}$$

The available data at a monitoring field include the coordinates of all the sensors and the measured arrival time to different sensors. The unknown entities are the coordinates of the MS source. In Eq. (18), a field pre-measured velocity is no longer necessary. The corresponding objective subdeterminant for each sensor can be confirmed in a similar way. By this way, a new objective function R of which the regression value is 0 can thus be defined as

$$\begin{aligned} R &= R_1 + R_2 + R_3 + \cdots + R_i + \cdots + R_n \\ &= \sum_{j=1}^{n} \{[(D_j - D_k)/(t_j - t_k) - (D_j - D_u)/(t_j - t_u)]^2 + \\ &\quad [(D_k - D_j)/(t_k - t_j) - (D_k - D_u)/(t_k - t_u)]^2 + \\ &\quad [(D_u - D_j)/(t_u - t_j) - (D_u - D_k)/(t_u - t_k)]^2\} \end{aligned} \tag{19}$$

The coordinates of the estimated MS source (x_0', y_0', z_0') can be calculated by iterations.

2) If $t_j = t_k$ (or $t_j = t_u$)

Considering the assumption that the wave velocities to the three nearest sensors have the same value, equating Eq. (8) and Eq. (9), it gives

$$\begin{aligned} & (x_j - x_0')^2 + (y_j - y_0')^2 + (z_j - z_0')^2 = (x_k - x_0')^2 + \\ & \quad (y_k - y_0')^2 + (z_k - z_0')^2 \end{aligned} \tag{20}$$

Reorganizing Eq. (20), it has

$$\begin{aligned} & (x_j - x_k)x_0' + (y_j - y_k)y_0' + (z_j - z_k)z_0' - \\ & \quad \frac{1}{2}(x_j^2 - x_k^2 + y_j^2 - y_k^2 + z_j^2 - z_k^2) = 0 \end{aligned} \tag{21}$$

Equation (21) is the middle plane equation between point (x_j, y_j, z_j) and point (x_k, y_k, z_k) in the three-dimensional space, and the problem of searching the MS source is then simplified into searching the source on the middle plane. And a new objective function by ignoring sensor j or sensor k can be adopted. When another neighbor sensor is considered, Eq. (19) can be used again as the objective function.

At the same time, the application conditions of the new velocity model should be noticed. First, the minimum number of sensors is four. Second, the number of sources and planes produced inside the sensors' array should be as many as possible.

4 Comparison of velocity models and error analysis

4.1 Comparison of velocity models

As shown in Fig. 1, there are four velocity models for identifying the micro-seismic location. For the convenience of analysis, the field measurement based single velocity model is called SFVM for short, and the inversion based single velocity model is denoted to be SIVM for short. The field measurement based multidirectional velocity model and the proposed multidirectional velocity in this work are denoted to be MFVM and MNVM for short, respectively. It can be found that different velocity models are based on different assumptions on stress wave propagation velocity from a MS source to sensors.

Figure 2 illustrates how the velocity models work, in which Sensor 1 to Sensor 7 and Source 1 to Source 3 are distributed, among which Source 1 is a calibration blasting test source for pre-measurement of the wave velocities, Source 2 is within the sensor's array while Source 3 is outside. Velocities from each source to

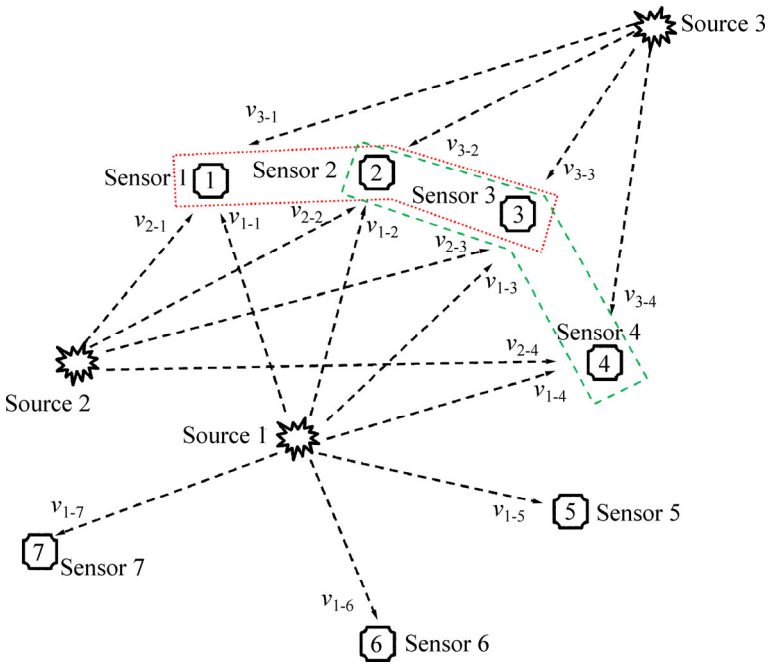

Fig. 2 Location principles based on different velocity models

different sensors are indicated in Fig. 2.

For the models of SFVM and SIVM, an assumption is made that the values of velocities from different sources to different sensors are the same, which means $v_{i\text{-}j}=C$ (i is the number of source, j is the number of sensor, and C is a constant). C is determined by field measurement for the SFVM model and taken as an additional unknown for the SIVM model, which is suitable only for homogeneous rock mass and it may cause a big error in a practical engineering application where various discontinuities always exist.

With respect to the MFVM model, the assumption is made that the velocities from different sources to some fixed sensors are the same, which means $v_{i\text{-}j}=C_j$ (i is the number of source, j is the number of sensor, and C_j is a constant). It can be assumed in Fig. 2 that $v_{1\text{-}1}=v_{2\text{-}1}=v_{3\text{-}1}=C_1$, $v_{1\text{-}2}=v_{2\text{-}2}=v_{3\text{-}2}=C_2$, $v_{1\text{-}3}=v_{2\text{-}3}=v_{3\text{-}3}=C_3$, ⋯. And C_j are obtained by field measurements which are more suitable for the case of similar stress propagation paths to the calibration blasting test, for example, from Source 1 and Source 2, the wave velocities to the sensors are more and less similar. For Source 3, the source is located outside the estimated region, and the wave propagation paths are different from those of Source 1, which may cause a significant error.

Based on the MNVM proposed in this work, each sensor j corresponds to an objective subdeterminant R_j. It is assumed that from a MS source to sensor j and two sensors k and u, the nearest sensors to sensor j have the same velocities. The wave velocity may vary for different sources, which can better approximate the actual velocity from each source to different sensors compared with three traditional models.

For the objective subdeterminant of R_j, it has $v_{i\text{-}j}=v_{i\text{-}k}=v_{i\text{-}u}$ (i is the number of source, sensor j is the sensor corresponding to R_j, and sensors k and u are the two nearest sensors to sensor j). And it can also be assumed in Fig. 2 that $v_{1\text{-}2}=v_{1\text{-}1}=v_{1\text{-}3}$ (sensors 1, 3 are the two nearest sensors to sensor 2) and $v_{1\text{-}3}=v_{1\text{-}2}=v_{1\text{-}4}$ (sensors 2, 4 are the two nearest sensors to sensor 3), ⋯. The coordinates of sources are obtained by different iteration methods based on the combined function of the objective subdeterminats. No matter where the source is and what the heterogeneity the rock mass has, the new multidirectional velocity model does not require field velocity pre-measurement and velocity inversion.

4.2 Error analysis

Micro-seismic monitoring for rock engineering using iterative velocity algorithms has the following possible errors.

1) Random error

Due to the heterogeneity of a rock mass, temperature change, rainfall and so on, a stress wave refracts and reflects at the discontinuities. The error caused by the heterogeneity of a rock mass is called random error, which exists in all the velocity models and it cannot be eliminated completely.

2) Method error

Considering that the wave velocities from different sources to different sensors vary, however, the SFVM and SIVM models both simplify the actual condition into a single velocity model; they cannot conform to the actual geological condition obviously. Moreover, the

deviation vector of coordinates is related to the deviation vector of the wave propagation velocity in the process of inversion for the SIVM model, resulting in further increase of the method error. Although the MFVM model takes different values in multiple directions, the assumption that the velocities from different sources to the same sensor are the same could introduce a big error. The MNVM model takes the actual condition into account, and the only assumption is that the velocities from a source to the nearest three sensors are the same during the iteration process. The error caused by the velocity models can be reduced by a suitable sensor distribution pattern, and this error by using the MNVM model is much smaller compared with that caused by the three traditional velocity models.

3) Measurement error

Considering that the rock mass structure is complicated, the wave propagation path of the calibration test can be very different from the one when a micro-seismic event actually occurs. The measured wave velocity may introduce errors in the analysis if the SFVM or MFVM model is used. The SIVM and MNVM models, however, do not have such errors.

4) Instrument error

The sensitivity and stability of the sensors may bring in an instrument error due to the limitations of the instrument itself. This error can be reduced by careful calibration of the instruments, although it is difficult to be completely avoided.

4.3 Comprehensive analysis

By analyzing the velocity models and their errors, potential levels of the errors from different methods are summarized in Table 1.

For an engineering rock mass, the four velocity models will all cause random error. Based on the above analysis, it can be drawn preliminarily that the errors introduced by the MNVM model will be the smallest compared to those from the other three velocity models. This can be proved by case studies in the following sections.

5 Verification

5.1 Numerical case overview

As shown in Fig. 3, an example model is set to verify the effectiveness of the proposed multidirectional velocity model. A cube array with eight sensor vertexes of A, B, C, D, E, F, G and H, three randomly selected internal sources of I, J and K, and three external sources L, M and N, are configured, and the coordinates of each point are given in Tables 2 and 3.

In order to simulate the difference of stress wave propagation velocity in different directions, the velocity from each source to each sensor is selected by random numbers with a mean of 5000 m/s and a measurement error of 1%, 3% and 5%, respectively. The arrival time of each sensor from sources with different velocity variations is shown in Tables 4 −6.

Three iterative algorithms, including the Levenberg-Marquardt method, the Gauss-Newton iteration method and the Simplex method are adopted to solve the non-linear least squares problem of the objective function. The Levenberg-Marquardt method is considered to be one of the most widely used damped least-squares (DLS) methods. The Gauss-Newton iteration method has been used to identify the MS source for a long time, and it has been called the Geiger method [18] in this field. The Simplex method was developed by NELDER and MEAD [23] and introduced into the field of MS location in late 1980s by PRUGGER and GENDZILL [22]. The first two methods solve the non-linear least squares by means of algebraic reconstruction technique, while the latter method searches the solution of non-linear least squares problem by the fixed rules.

For example, the process with the Simplex method involves four general steps:

1) Setting an initial Simplex figure;

2) Calculating errors for vertices;

3) Moving Simplex figures;

4) Examining the status of convergence.

An initial Simplex figure has to be set firstly, and then by rolling through the error space, expanding, shrinking, contracting and turning towards the minimal error point of the space. The movement of the Simplex figure is decided by the error distribution at its vertex, which is calculated each time when the Simplex figure is reshaped.

These three methods are considered to be the most commonly used methods at present. Compared with those using three traditional velocity models and the new model, 24 examples are set up to verify the velocity anisotropy range of 1%, 3% and 5%, as listed in Table 7.

Table 1 Error summary of different kinds of velocity models

Velocity model	Direction of velocity	Origin of velocity parameter	Random error	Method error	Measure error	Instrument error
SFVM	Single	Field measurement	Existent	Big	Small	Middle
MFVM	Multiple	Field measurement	Existent	Big	Small	Big
SIVM	Single	Velocity inversion	Existent	Big	Non-existent	Small
MNVM	Multiple	Without measurement and	Existent	Small	Non-existent	Small

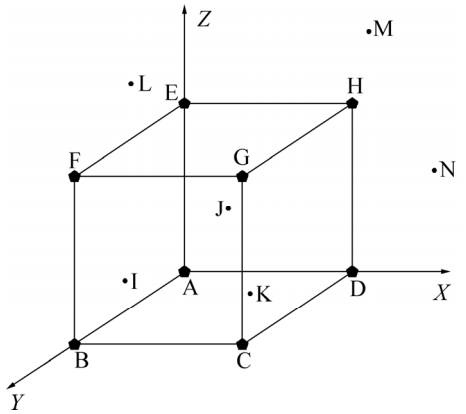

Fig. 3 Calculation model

Table 2 Coordinates of sensors

Sensor	*X*/m	*Y*/m	*Z*/m
A	0	0	0
B	0	1000	0
C	1000	1000	0
D	1000	0	0
E	0	0	1000
F	0	1000	1000
G	1000	1000	1000
H	1000	0	1000

Table 3 Coordinates of sources

Sensor	*X*/m	*Y*/m	*Z*/m
I	253	756	342
J	497	329	751
K	624	594	103
L	675	1328	1745
M	1681	974	1950
N	2489	1567	1436

Table 4 Arrival times of each sensor from sources (1% for velocity anisotropy range) (Unit: ms)

Sensor	Source					
	I	J	K	L	M	N
A	172.46	191.37	173.88	463.51	554.96	649.41
B	98.08	225.06	151.22	382.20	520.14	588.14
C	172.44	226.50	112.57	359.57	417.30	431.57
D	222.40	193.93	141.25	443.36	457.64	519.03
E	206.32	129.45	248.25	336.49	429.09	595.86
F	150.71	176.03	235.49	210.23	383.91	520.03
G	172.79	226.05	112.13	363.19	412.31	428.99
H	251.51	131.16	227.93	312.02	303.69	439.27

5.2 Result analysis

The results of the 24 examples with different velocity variation range and measurement errors are plotted in Figs. 4−6. They show that:

Table 5 Arrival times of each sensor from sources (3% for velocity anisotropy range) (Unit: ms)

Sensor	Source					
	I	J	K	L	M	N
A	171.10	196.87	173.53	448.12	553.85	649.41
B	95.97	230.13	150.01	375.40	511.86	597.74
C	176.34	224.70	111.24	351.18	422.42	423.90
D	220.21	192.77	138.50	434.67	467.00	515.93
E	212.26	129.71	251.26	327.87	429.09	578.47
F	147.43	173.92	239.85	211.92	383.91	505.81
G	169.37	226.05	114.64	357.44	422.42	426.43
H	255.10	131.96	228.39	312.02	296.59	444.59

Table 6 Arrival times of each sensor from sources (5% for velocity anisotropy range) (Unit: ms)

Sensor	Source					
	I	J	K	L	M	N
A	166.50	190.61	171.13	453.44	569.90	635.54
B	96.54	231.08	157.23	384.52	538.63	612.75
C	165.13	229.74	113.03	355.33	405.83	414.88
D	225.10	188.98	146.80	466.70	440.00	521.11
E	200.72	124.70	257.50	324.68	444.98	600.67
F	144.57	183.44	235.49	213.20	385.44	540.65
G	175.98	236.50	109.29	374.49	426.79	447.79
H	263.16	124.16	231.64	325.73	315.66	464.24

1) As the velocity deviation range changes from 1% to 3% and 5%, the errors of the estimated MS location for all the 24 cases become drastically larger. As shown in Fig. 4, the location errors for Cases 1, 2 and 3 of source K are 9.28 m, 20.34 m and 38.16 m, respectively, when the velocity deviation range is 1%. In Fig. 5, these errors change into 15.92 m, 36.28 m and 67.85 m, respectively, when velocity deviation range is 3%. The errors further increase to 28.39 m, 41.07 m and 102.41 m, respectively, when the velocity deviation range becomes 5%, as seen in Fig. 6. Similar trend can be found for the rest 21 cases in Figs. 4−6, which means that the velocity deviation is the key influence factor in locating the MS source.

2) The errors based on the three traditional velocity models appear to be more significant than those based on the proposed MNVM model. When the MNVM velocity model is applied, the error is less sensitive no matter which iterative algorithm is adopted. The MNVM model assumes the same velocity from a MS to three nearest sensors, which is closer to the actual site situation compared with traditional models. Moreover, it not only avoids the error due to pre-measurement of the wave velocity compared with the SFVM and MFVM models, but also avoids the method error caused by the velocity

Table 7 Summary of location methods used in this example

Velocity model	Case No.	Measured error range/%	Iterative algorithm
SFVM	1	1	Levenberg-Marquardt method
	2	3	
	3	5	
	4	1	Gauss-Newton iteration method
	5	3	
	6	5	
	7	1	Simplex method
	8	3	
	9	5	
MFVM	10	1	Levenberg-Marquardt method
	11	3	
	12	5	
	13	1	Gauss-Newton iteration method
	14	3	
	15	5	
	16	1	Simplex method
	17	3	
	18	5	
SIVM	19	—	Levenberg-Marquardt method
	20		Gauss-Newton iteration method
	21		Simplex method
MNVM	22	—	Levenberg-Marquardt method
	23		Gauss-Newton iteration method
	24		Simplex method

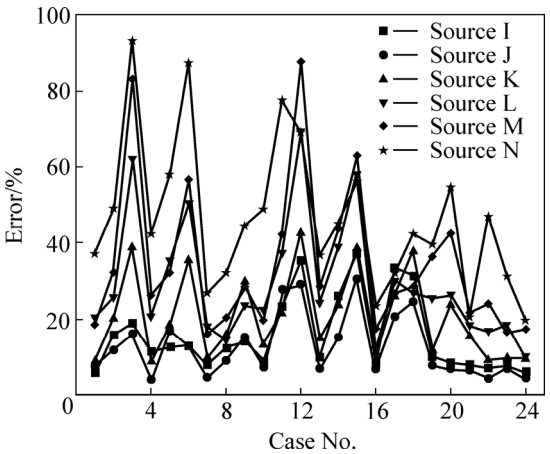

Fig. 4 Comparison of location errors for different cases (1% for velocity anisotropy range)

inversion in the SIVM model. It is shown that MNVM is not sensitive to the velocity deviation in different directions during the process of iteration.

3) Figures 4−6 also show that the Simplex method has better performance compared with the Gauss-Newton iteration method and the Levenberg-Marquardt method, especially when the sources are outside the sensors array

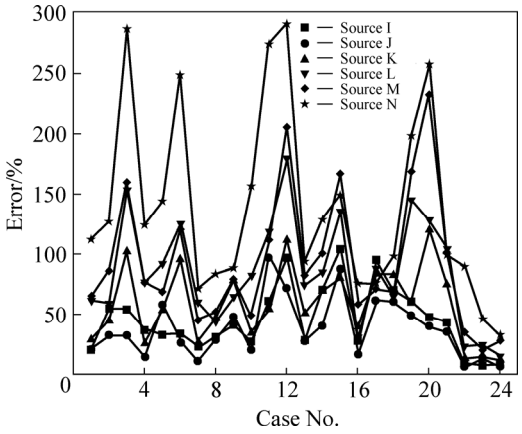

Fig. 5 Comparison of location errors for different cases (3% for velocity anisotropy range)

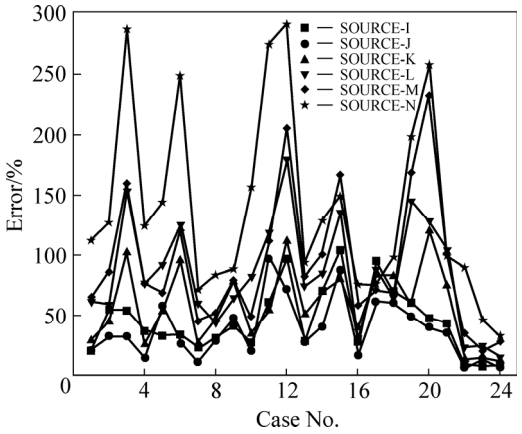

Fig. 6 Comparison of location errors for different cases (5% for velocity anisotropy range)

sensors array. Using the same velocity model, the iterative algorithm has less effect if an MS source is within the sensors' array. However, for the sources outside the sensors' array, for example, the sources L, M and N, the final positioning errors are obviously different based on different iterative algorithms. The Levenberg-Marquardt method introduces the largest error while the Simplex method gives the lowest.

4) It can also been seen from Figs. 4 to 6 that the measurement velocity error affects the final error apparently based on SFVM and MFVM. For the change of the measurement velocity error, the final error of Cases 1−3 and Cases 10−12 based on the Levenberg-Marquardt iteration method are much larger than those of Cases 4−6 and Cases 13−15 based on Gauss-Newton iterative method, and also those of Cases 7−9 and Cases 16−18 based on the Simplex method. It is shown that the sequence of influence level of different iterative algorithms is Levenberg-Marquardt iteration method> Gauss-Newton iteration method>Simplex method.

Based on the comprehensive analysis of the 24 cases, it is verified that the proposed multidirectional velocity model with the Simplex iteration method always

gives the lowest error. It not only effectively solves the coordinates of sources whether the source is within the sensors' array or not, but also is insensitive to the velocity deviation in different directions.

5.3 Engineering application

The new model is then applied to three blasting tests in the Dongguashan Mine [25], where a micro-seismic monitoring system is set up with 16 sensors.

Coordinates of sensors and triggered times by sensors are listed in Table 8. The calculated locations and computed results of the blasting events based on SIVM with the time residual objective function (TT method), SIVM with the time residual cross objective function (TD method) and the proposed MSVM (new method) are shown in Fig. 7 and Table 9.

Table 8 Coordinates of sensors and triggered times by sensors

Number of sensor	Direction/m			Arrival time to sensors/ms		
	X	*Y*	*Z*	Event 1	Event 2	Event 3
Site 1	84345.73	22474.0	−678.01	31.214136	0.563835	45.26793
Site 2	84157.08	22717.2	−737.28			45.26493
Site 3	84256.71	22587.9	−682.80	31.225969	0.574668	45.25826
Site 4	84493.74	22395.4	−653.02	31.210303	0.567501	
Site 5	84299.94	22861.7	−764.74			45.26118
Site 6	84377.81	22755.5	−722.01	31.222942	0.566903	45.24801
Site 7	84487.86	22612.0	−704.33	31.195608	0.547570	45.25868
Site 8	84580.14	22489.6	−693.73	31.196942	0.556570	
Site 9	84591.12	22453.2	−862.58	31.206442	0.556775	
Site 10	84349.47	22271.4	−862.79			
Site 11	84429.88	22332.3	−863.16	31.226608	0.573108	
Site 12	84509.80	22391.8	−862.91	31.213275	0.561441	
Site 13	84076.11	22705.4	−862.89			45.28031
Site 14	84182.39	22775.1	−862.38			45.26864
Site 15	84259.16	22840.2	−862.04			45.26714
Site 16	84307.19	22943.1	−860.87			45.27964

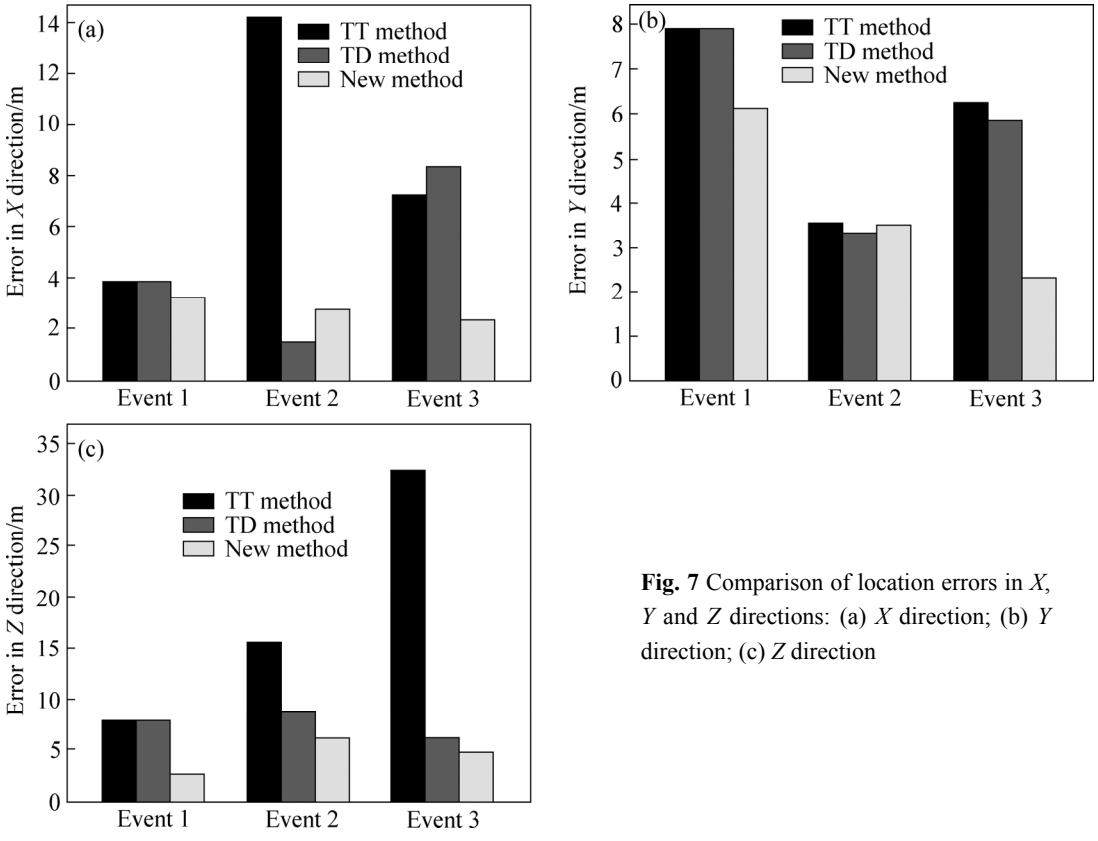

Fig. 7 Comparison of location errors in *X*, *Y* and *Z* directions: (a) *X* direction; (b) *Y* direction; (c) *Z* direction

Table 9 Locations and computed results of blasting

Event	Direction	Blasting coordinate	Computed coordinate	Error	Error computed by new method/m	Error computed by TD method/m	Error computed by TT method /m
1	*X*	84528.4	84531.2594	−2.8594	6.7540	10.9323	10.9935
	Y	22556.2	22550.3166	5.8834			
	Z	−753.2	−751.5191	−1.6809			
2	*X*	84479	84481.3952	−2.3952	6.6574	8.4000	20.3198
	Y	22570	22573.2857	−3.2857			
	Z	−814.4	−819.6715	5.2715			
3	*X*	84359	84357.0184	1.9816	4.8780	11.1376	32.4625
	Y	22673	22670.9023	2.0977			
	Z	−795.5	−799.4329	3.9329			

From Fig. 7 and Table 9, the following results can be found:

1) The results based on the new model have good agreement with the results of the three blasting tests. Compared with the TT method and the TD method, the errors from the new method are reduced from 10.9935 m and 10.9323 m to 6.7540 m for Event 1, 20.3198 m and 8.4000 m to 6.6574 m for Event 2, and 32.4625 m and 11.1376 m to 4.8780 m for Event 3. The maximum reduction of the error is 84.97% for Event 3.

2) Different from the TD method and TT method, the errors in various directions based on the new method are all lower than 10 m for all the three events, which is acceptable for the engineering application.

3) The new method shows good performance in the aspects of accuracy and stability for the three events, which further verifies the validity of this model.

6 Conclusions

1) A new multidirectional velocity model is proposed which does not require field pre-measurement of the wave propagation velocity and velocity inversion. The results of 24 case studies and an engineering application verify that the proposed model has advantage over the three traditional velocity models in more accurately locating micro-seismic sources.

2) The error when identifying the micro-seismic source is significantly affected by the velocity deviation. Its influence is much more obvious than other factors. Considering that the laws of the velocity deviation are difficult to be completely avoided, choosing a suitable velocity model to reduce its influence is important.

3) The new multidirectional velocity model assumes that the wave propagation velocities from a micro-seismic source to three nearest sensors are the same. Since the proposed velocity model does not require pre-measurement of the wave velocity and velocity inversion, the measurement error and method error are reduced compared to the three traditional velocity models. The 24 numerical examples and the engineering application indicate that the new velocity model with Simplex method always gives the lowest error.

4) It is also found that the new velocity model with the Simplex method has good stability when the velocity deviation changes from 1% to 3%. And both the internal and external sources for the sensors array can be effectively searched based on the proposal velocity model.

Acknowledgment

The first author would like to thank the support of the China Scholarship Council and the host organization the University of Western Australia for his one year visit.

References

[1] HARDY H R. Acoustic emission/microseismic activity: Volume 1: Principles, techniques and geotechnical applications [M]. United Kingdom, Abingdon: Taylor & Francis, 2003: 1−27.

[2] WANG Hong-liang, GE Mao-chen. Acoustic emission/microseismic source location analysis for a limestone mine exhibiting high horizontal stresses [J]. International Journal of Rock Mechanics and Mining Sciences, 2008, 45(5): 720−728.

[3] XU Nu-wen, DAI Feng, LIANG Zheng-zhao, ZHOU Zhong, SHA Chun, TANG Chun-an. The dynamic evaluation of rock slope stability considering the effects of microseismic damage [J]. Rock Mechanics and Rock Engineering, 2014, 47(2): 621−642.

[4] MA Ke, TANG Chun-an, XU Nu-wen, LIU Feng, XU Jing-wu. Failure precursor of surrounding rock mass around cross tunnel in high-steep rock slope [J]. Journal of Central South University, 2013, 20(1): 207−217.

[5] WANG Hong-qiang, XIA Hong-en, CHENG Yong-qiang, WANG Lu-lu. An adaptive waveform-detection threshold joint optimization method for target tracking [J]. Journal of Central South University, 2013, 20(11): 3057−3064.

[6] ALBRIGHT J N, PEARSON C F. Acoustic emissions as a tool for hydraulic fracture location: Experience at the Fenton Hill Hot Dry Rock site [J]. Society of Petroleum Engineers Journal, 1982, 22(4): 523−530.

[7] HUTTON P H, SKORPIK J R. A simplified approach to continuous

AE monitoring using digital memory storage [C]// Proceedings of Third Acoustic Emission Symposium. Tokyo, Japan, 1976: 2−6.

[8] INGLADA V. The calculation of the stove coordinates of a Nahbebens [J]. Gerlands Beitrage zur Geophysik, 1928(19): 73−98. (in Germany)

[9] LEIGHTON F, BLAKE W. Rock noise source location techniques [M]. United Kingdom, Abingdon: Taylor & Francis, 1970: 1−18.

[10] TAYLOR H L. The L1 norm in seismic data processing [M] Developments in Geophysical Exploration Methods. Netherlands: Springer, 1981: 53−76.

[11] ANDERSON K R. Robust earthquake location using M-estimates [J]. Physics of the Earth and Planetary Interiors, 1982, 30(2): 119−130.

[12] BULAND R. The mechanics of locating earthquakes [J]. Bulletin of the Seismological Society of America, 1976, 66(1): 173−187.

[13] GEIGER L. Probability method for the determination of earthquake epicenters from the arrival time only (translated from Geiger's 1910 German article) [J]. Bulletin of St. Louis University, 1912, 8(1): 56−71.

[14] CHRISTY J J. A Comparative study of the 'miner' and least squares location techniques as used for the seismic location of trapped coal miners [D]. Pennsylvania State University, 1982.

[15] STRANG G. On the construction and comparison of difference schemes [J]. SIAM Journal on Numerical Analysis, 1968, 5(3): 506−517.

[16] VANDECAR J C, CROSSON R S. Determination of teleseismic relative phase arrival times using multi-channel cross-correlation and least squares [J]. Bulletin of the Seismological Society of America, 1990, 80(1): 150−169.

[17] MENKE W. Using waveform similarity to constrain earthquake locations [J]. Bulletin of the Seismological Society of America, 1999, 89(4): 1143−1146.

[18] LI Xi-bing, DONG Long-jun. Comparison of two methods in acoustic emission source location using four sensors without measuring sonic speed [J]. Sensor Letters, 2011, 9(5): 2025−2029.

[19] AKI K, LEE W H K. Determination of three-dimensional velocity anomalies under a seismic array using first P arrival times from local earthquakes: 1. A homogeneous initial model [J]. Journal of Geophysical Research, 1976, 81(23): 4381−4399.

[20] PAVLIS G L, BOOKER J R. The mixed discrete-continuous inverse problem: Application to the simultaneous determination of earthquake hypocenters and velocity structure [J]. Journal of Geophysical Research: Solid Earth (1978–2012), 1980, 85(B9): 4801−4810.

[21] THURBER C H. Nonlinear earthquake location: theory and examples [J]. Bulletin of the Seismological Society of America, 1985, 75(3): 779−790.

[22] PRUGGER A F, GENDZWILL D J. Microearthquake location: A nonlinear approach that makes use of a simplex stepping procedure [J]. Bulletin of the Seismological Society of America, 1988, 78(2): 799−815.

[23] NELDER J A, MEAD R. A simplex method for function minimization [J]. Computer Journal, 1965, 7(4): 308−313.

[24] WALDHAUSER F, ELLSWORTH W L. A double-difference earthquake location algorithm: Method and application to the northern Hayward fault, California [J]. Bulletin of the Seismological Society of America, 2000, 90(6): 1353−1368.

[25] DONG Long-jun, LI Xi-bing, TANG Li-zhong, GONG Feng-qiang. Mathematical functions and parameters for microseismic source location without premeasuring speed [J]. Chinese Journal of Rock Mechanics and Engineering, 2011, 30(10): 2057−2067. (in Chinese)

(Edited by FANG Jing-hua)